Symmetry-Reduced Algebraic Selective Harmonic Elimination for Cascaded H-Bridge Converters with Unequal DC Source Levels

Jared Miller
Chair of Mathematical Systems Theory
University of Stuttgart
Stuttgart, Germany
jared.miller@imng.uni-stuttgart.de

Nicolás Estay
Department of Electrical Engineering
Universidad Técnica Federico Santa María
Valparaíso, Chile
nicolas.estay@usm.cl

Petros Karamanakos
Faculty of Inf. Technol. and Commun. Sciences
Tampere University,
Tampere, Finland
p.karamanakos@ieee.org

Alejandro Angulo
Department of Electrical Engineering
Universidad Técnica Federico Santa María
Valparaíso, Chile
alejandro.angulo@usm.cl

***Abstract*— Low-order current harmonics are undesirable in power converter and electric drive systems because they are difficult to filter out effectively. Selective harmonic elimination (SHE) is a modulation-based method commonly employed to suppress specific harmonic components. Computing the switching time instants (commonly expressed as switching angles) of SHE pulse patterns, however, remains challenging because it requires solving a nonlinear system of equations. This paper proposes a symmetry-reduced formulation based on partition-compatible elementary symmetric polynomials that improves computational tractability and enables the computation of all solutions of the resulting polynomial system. The proposed framework is developed for cascaded H-bridge converters with unequal dc cell voltages, thereby addressing a more general setting than the equal-voltage case commonly considered in the literature. Numerical results verify the effectiveness of the method in eliminating the targeted harmonics.**

***Index Terms*—Multilevel converters, selective harmonics elimination (SHE), algebraic methods, symmetry**

I. Introduction

Power converters are switching devices that inherently generate harmonic distortions. Low-order harmonics are particularly undesirable because they cannot be filtered effectively. In electrical drives, such harmonics can produce low-order torque pulsations that cause shaft vibrations [1], whereas in grid-connected converters, harmonic standards impose stringent limits on allowable distortion levels [2].

A software-based approach for harmonic suppression is pulse width modulation (PWM). Selective harmonic elimination (SHE) [3], [4], [5], [6] is a well-established method for eliminating specific harmonic components. In SHE for a two-level converter, a pulse pattern with quarter- and half-wave symmetry (QaHWS) is parameterized by k switching angles, which determine the switching time instants over a fundamental period. These angles are computed offline such that the fundamental component attains the desired amplitude, corresponding to the modulation index, while $k-1$ selected harmonics are eliminated. This leads to a system of k nonlinear equations in the cosines of the switching angles [7], [8]. Because this system is nonlinear, multiple solutions may exist, and computing all of them is generally challenging. However, the resulting polynomial system exhibits permutation symmetry in the ordering of its roots. This property allows symmetry-reduction techniques from invariant theory, based on elementary symmetric polynomials [9], to reduce the complexity of SHE root computation [10]. When multiple feasible solutions are available, one may subsequently select the solution that offers the most favorable trade-off with respect to additional performance criteria, such as harmonic distortion or dc-link voltage utilization.

For multilevel converters, the SHE problem becomes more involved because the sequence of converter voltage levels forming the pulse pattern must be determined. The work in [11] addresses this issue by using the signs of the SHE roots to generate the voltage-level sequence and switching angles simultaneously. However, when the converter dc voltage levels are unequal, the symmetry properties exploited in the equal-voltage case are no longer fully applicable. To address this more general setting, [12] extends the universal formulation of [11] to unequal SHE and computes all roots using path tracking [13], but without symmetry reduction. The work in [14] formulates unequal SHE as a branch-and-bound global optimization problem, while [15] employs heuristic search techniques. In [16], explicit solutions are derived for special unequal dc multilevel SHE-based patterns. The work in [17] rapidly computes a single SHE solution for equal or exponentially decaying dc voltage sources by solving a linear matrix equation.

Motivated by the above, this work focuses on computing *all* solutions of the unequal SHE problem for multilevel cascaded H-bridge (CHB) converters, in which the dc-source voltages of the individual H-bridge cells are not necessarily equal [18, Ch. 7]. To this end, the problem is decomposed into cases determined by how the switching angles are distributed among groups of cells having identical dc voltage levels. This decomposition reflects a restricted permutation symmetry: switching angles may be permuted within each equal-voltage group, but not across groups associated with different dc voltage levels. This partition-compatible symmetry is exploited by introducing elementary symmetric polynomials within each group, thereby obtaining a symmetry-reduced formulation of the unequal SHE equations. The resulting reduced polynomial systems are then solved using homotopy continuation methods [13], [19], allowing the computation of all solutions of the unequal SHE problem. Numerical results demonstrate the effectiveness of the proposed computational approach.

II. Preliminaries

This section first introduces the power electronic system used as a case study. Subsequently, the theoretical background of SHE is presented.

A. Notation

The set of real numbers is $\mathbb{R}$ and the set of natural numbers (nonnegative integers including zero) is $\mathbb{N}$. The set of n-dimensional multi-indices is $\mathbb{N}^n$. The cardinality (number of elements) of a discrete set L is $|L|$. The degree of a multi-index $\beta \in \mathbb{N}^r$ is $|\beta| = \sum_{i=1}^r \beta_i$. The set of multi-indices with degree equal to d is $\mathbb{N}_d^r$ with $|\mathbb{N}_d^r| = \binom{r+d-1}{r-1}$. As an example, $\mathbb{N}_3^2 = \{(3,0),(2,1),(1,2),(0,3)\}$ with $|\mathbb{N}_3^2| = 4$. The univariate Chebyshev polynomials of the first kind at degree $\ell \in \mathbb{N}$ are defined by the recurrence $T_0(x) = 1,\ T_1(x) = x,\ T_{\ell+1}(x) = 2xT_\ell(x) - T_{\ell-1}(x)$, and satisfy the property $\cos(\ell\theta) = T_\ell(\cos(\theta))$ for all $\ell \in \mathbb{N},\ \theta \in [0, 2\pi]$.

B. Power Electronic System

All signals in this paper are assumed to be 2π-periodic, with fundamental frequency $f_1 = 1/T_1$, where T_1 is the fundamental period. A CHB converter consists of N_c H-bridge cells, each with a nonnegative dc supply voltage E_j for $j \in \{1, \ldots, N_c\}$. The output voltage of each cell can be modeled with the switch position $\sigma_j \in \{-1, 0, 1\}$ for $j \in \{1, \ldots, N_c\}$. The number of unique cell values in E is r. The converter has equal dc levels if all per-cell voltages E_j are equal ($r = 1$). The output voltage of the converter is $v_{\text{out}} = \sum_{j=1}^{N_c} \sigma_j (E_j/2)$.

Example 2.1: As an example, consider the three-cell converter in Fig. 1 with $E_1 = 2\,\text{kV}$, $E_2 = 2\,\text{kV}$, and $E_3 = 3\,\text{kV}$. These dc voltages will be expressed as $E_1 = 2$, $E_2 = 2$, and $E_3 = 3$ in normalized voltage values when performing SHE.

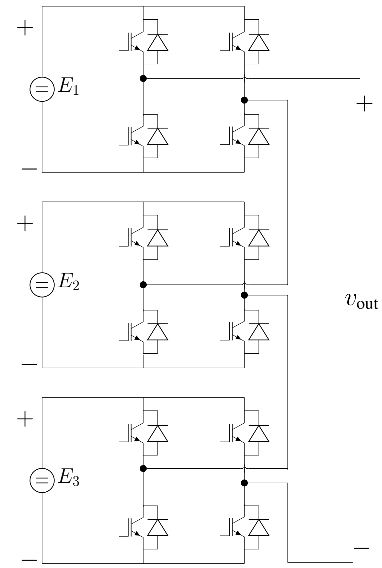

Fig. 1: CHB converter with $E_1 = 2$, $E_2 = 2$, and $E_3 = 3$

C. Pulse Patterns and SHE

A 2π-periodic switching signal (i.e., pulse pattern) $u(\theta)$ with k switching transitions is described by switching angles $\alpha \in [0, 2\pi]^k$ and levels $u \in \mathbb{R}^{k+1}$:

$$u(\theta) = \begin{cases} u^0 & \theta \in [0, \alpha^1) \\ u^i & \theta \in [\alpha^i, \alpha^{i+1}),\ i \in 1, \ldots, k-1 \\ u^k & \theta \in [\alpha^k, 2\pi]. \end{cases} \tag{1}$$

The signal is assumed to satisfy the following symmetries:

$$\text{Full-wave} \qquad u(\theta + 2\pi) = u(\theta) \qquad \forall\theta \in [0, 2\pi] \tag{2a}$$
$$\text{Half-wave} \qquad u(\theta + \pi) = -u(\theta) \qquad \forall\theta \in [0, 2\pi] \tag{2b}$$
$$\text{Quarter-wave} \qquad u(\theta) = u(\pi - \theta) \quad \forall\theta \in [0, \pi]. \tag{2c}$$

A pulse pattern $u(\theta)$ with QaHWS also fulfills $u(0) = u(\pi) = u(2\pi) = 0$. The *pulse number* of a pattern with QaHWS is $d := k/4$. Such a pattern is uniquely determined by the d switching angles $\{\alpha^i\}_{i=1}^d$ and the sequence of output voltage levels (i.e., switching sequences) $\{u^i\}_{i=0}^d$ in the first quarter of the fundamental period. Moreover, $u(\theta)$ admits the Fourier series $u(\theta) = \sum_{\ell=1}^\infty b_\ell \sin(\ell\theta)$ with coefficients

$$b_\ell = \begin{cases} \frac{4}{\ell\pi} \sum_{i=1}^k (u^{i-1} - u^i)\cos(\ell\alpha^i) & \ell \text{ odd} \\ 0 & \ell \text{ even.} \end{cases}$$

Example 2.2: The switching angles $\{\alpha_i\}$ and levels $\{u_i\}$ that describe a QaHWS pattern for the CHB converter in Fig. 1 with $d = 4$ are

$$\{\alpha_i\}_{i=1}^4 = \{0.3812, 0.9753, 1.3100, 1.3659\}, \tag{3a}$$
$$\{u_i\}_{i=0}^4 = \{0, 1, 2, 3.5, 2\}. \tag{3b}$$

Fig. 2 illustrates this pattern and the resultant output current $I(\theta)$ assuming a purely inductive load.

To generate a QaHWS pulse pattern using SHE, one solves a system of polynomial equations in the cosines of the switching

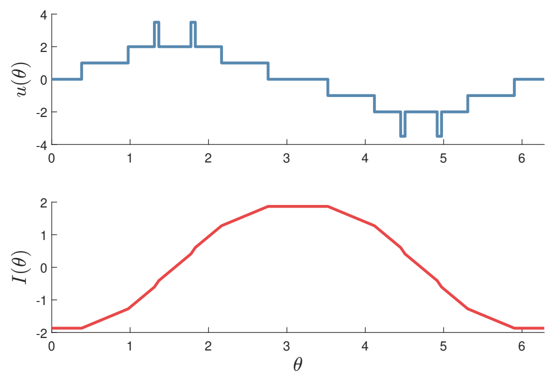

Fig. 2: Pulse pattern (3) and output current assuming an inductive load

angles, defined as $c^i := \cos(\alpha^i)$ for $i \in \{1, \ldots, d\}$ [4], [5], [7]. Specifically, SHE targets the harmonic orders contained in the index set

$$H \subset (1, 5, 7, 11, 13, \ldots) \qquad |H| = d. \tag{4a}$$

Triplen (i.e., common-mode) voltage harmonics are not considered, since for a balanced wye-connected load with floating neutral they do not contribute to the load current harmonics. Given a fixed level sequence $\{u^i\}_{i=0}^d$ with differences $\{\Delta u_i\}_{i=1}^d = \{u^i - u^{i-1}\}_{i=1}^d$, the QaHWS SHE problem takes the form

$$b_1 = \textstyle\sum_{i=1}^d -\Delta u^i c_i = M\frac{\pi}{4} \tag{5a}$$
$$b_\ell = \textstyle\sum_{i=1}^d -\Delta u^i T_\ell(c_i) = 0 \qquad \forall \ell \in H \setminus 1, \tag{5b}$$

where M denotes the amplitude of the desired fundamental voltage component, i.e., the amplitude of the reference signal $M\sin(\theta)$. It is therefore not a dimensionless modulation index, but a voltage-amplitude quantity expressed in the same normalization as the converter voltage levels. If multiple solutions to (5) exist, a pulse pattern may be selected according to additional performance criteria. Example criteria include the maximum common-mode component over one fundamental period and the weighted differential-mode distortion, respectively defined as

$$J_{\text{cm}} = \max_{\theta \in [0, 2\pi]} \tfrac{1}{3}|u(\theta) + u(\theta + \tfrac{2\pi}{3}) + u(\theta + \tfrac{4\pi}{3})|, \tag{6a}$$

$$J_{\text{TDD}} = \sqrt{\sum_{\ell \neq 1,\ 3 \nmid \ell} \frac{b_\ell^2}{\ell^2}}. \tag{6b}$$

The quantity J_{TDD} serves as a proxy for the current total demand distortion (TDD), to which it is proportional, since

$$\text{TDD}^{3\varphi} = \frac{1}{\sqrt{2} I_{\text{nominal}} \omega_1 L_{\text{load}}} \frac{E_{\text{dc}}}{2} J_{\text{TDD}}, \tag{7}$$

where I_{nominal} is the rated current, L_{load} the load inductance, and $E_{\text{dc}} = \sum_{j=1}^{N_s} = E$ the total dc voltage.

The system in (5) can be simplified using the identity $\cos(\pi - \theta) = -\cos(\theta)$ and noting that T_ℓ is an odd polynomial whenever ℓ is odd [7], [11]. In particular, (5) can be represented using variables $\{\tilde{c}_i\}_{i=1}^d$ as

$$b_1 = \textstyle\sum_{i=1}^d -|\Delta u^i| \tilde{c}_i = M\frac{\pi}{4} \tag{8a}$$
$$b_\ell = \textstyle\sum_{i=1}^d -|\Delta u^i| T_\ell(\tilde{c}_i) = 0 \qquad \forall \ell \in H \setminus 1. \tag{8b}$$

Any root $\tilde{c}_i$ of (8) can then be mapped to a switching angle α_i and switch position σ_i as

$$(\alpha_i, \sigma_i) = \begin{cases} (\cos^{-1}(\tilde{c}_i), |\Delta u_i|) & \tilde{c}_i \geq 0 \\ (\pi - \cos^{-1}(\tilde{c}_i), -|\Delta u_i| & \tilde{c}_i < 0. \end{cases} \tag{9}$$

This recovery method is the *unified formulation* of multilevel SHE [11], and it was extended to unequal dc voltage levels in [12].

TABLE I: Parameters for SHE with unequal dc voltage levels

Symbol	Description
E	Per-cell dc voltages
M	Amplitude of the first sine harmonic
H	Index set for SHE in (4)

III. SHE for Unequal DC Levels

To attain all solutions of the unequal dc-supply SHE problem (unequal SHE), the SHE system for (5) must be solved with respect to all possible d-length QaHWS switching level sequences $\{u^i\}_{i=0}^d$. This search will be accomplished by solving the SHE problem multiple times based on a partitioning of paths. The unequal SHE problem is completely described by the parameters in Table I, in which the pulse number d satisfies $d = |H|$.

Problem 3.1 (Unequal SHE): Given parameters in Table I, find all patterns $\mathcal{T} = (\{u\}_{i=0}^d, \{\alpha\}_{i=1}^d)$ that are feasible for the SHE system (5) and could be generated by the CHB converter.

The set of patterns returned by solving Problem 3.1 can be pruned by considering physical or performance constraints such as bounds on maximal current TDD, common-mode voltage, semiconductor power losses, and minimal angular intervals between consecutive switches (interlocking time).

A. Unified Formulation for Partitioned Unequal SHE

We first partition the set of admissible switching sequences that can be generated by a CHB converter. Let $(\tilde{E}_j)_{j=1}^r$ denote the unique elements of E sorted in increasing order, in which each element $\tilde{E}_j$ has an associated multiplicity m_j in E. For each multi-index $\gamma \in \mathbb{N}_d^r$, we denote a tuple $\mathcal{O}_\gamma = (\tilde{E}_j, m_j, \gamma)_{j=1}^r$ comprising the dc cell voltage, the multiplicity, and the number of switches performed by the cell-type within the first quarter period.

We define a γ-partitioned polynomial system in the variables $c_{j\nu}$ for each $\nu \in \{1, \ldots \gamma_j\}$ and $j \in \{1, \ldots r\}$. The γ-partitioned polynomial system for SHE is

$$\textstyle\sum_{j=1}^r \frac{\tilde{E}_j}{2} \left(\sum_{\nu=1}^{\gamma_j} c_{j\nu}\right) = M\frac{\pi}{4} \tag{10a}$$
$$\textstyle\sum_{j=1}^r \frac{\tilde{E}_j}{2} \left(\sum_{\nu=1}^{\gamma_j} T_\ell(c_{j\nu})\right) = 0 \qquad \forall \ell \in H \setminus 1. \tag{10b}$$

The system in (10) is an instance of the unified formulation from (8) [12] with respect to the voltage step values $|\Delta u|$ that are constrained to lie in E.

B. Symmetry Reduction and Solution Recovery

The polynomial system in (10) admits a symmetry structure: each index ν of the partition is invariant under permutations of its elements. We can use invariant theory to decompose (10) using elementary symmetric polynomials [9]. For each group $j \in \{1, \ldots, r\}$, we define symmetric polynomials $\{e_{\nu j}\}$ derived from $c_{j\nu}$ as

$$\begin{aligned} & e_{j0}(x) = 1, \qquad e_{j\gamma_j} = \textstyle\prod_{\nu=1}^{\gamma_j} c_{j\nu}, && (11) \\ & e_{j\nu}(x) = \textstyle\sum_{\beta_1 < \beta_2 < \ldots < \beta_\nu} c_{j\beta_1} c_{j\beta_2} \ldots c_{\beta_n u} \quad 1 \le \nu < \gamma_j, \\ & e_{j\nu}(x) = 0 \qquad\qquad \nu > \gamma_j. \end{aligned}$$

There exist unique polynomials $g_{j,\ell}(e_{j1}, \ldots e_{j\gamma_j})$ for each $j \in \{1, \ldots, r\}$ such that (10) can be written as

$$\textstyle\sum_{j=1}^{r} \frac{\tilde{E}_j}{2} e_{j1} = M\frac{\pi}{4}, \quad \forall \ell \in H \setminus 1 : \sum_{j=1}^{r} g_{j,\ell}(e_j) = 0. \tag{12}$$

Given a solution (e_j^*) that solves (12), we discard e^* if any element of e^* is complex. We then extract plausible candidates for angle cosines by finding the roots of a monic polynomial

$$t^{\gamma_j} + t^{\gamma_j - 1} e_{j1}^* + t^{\gamma_j - 2} e_{j2}^* + \ldots + t e_{j\ \gamma_j - 1}^* + e_{j\gamma_j}^*. \tag{13}$$

Letting $c_{j\nu}^*$ be the roots of the polynomial in t in (13) with respect to the dc voltage E_j, recovery proceeds if each element of c^* is real and has absolute value less than or equal to one. This process is based on the solution extraction procedure in [10] for SHE with equal dc sources.

We then apply the universal formulation from [12] to recover pulse patterns from $c_{j\nu}^*$. As an example, we create a tuple out of a switching angle α in terms of a sign σ.

$$(\sigma_{j\nu}, \alpha_{j\nu}) := \begin{cases} (1, \cos^{-1}(c_{j\nu}^*)) & c_{j\nu}^* \ge 0 \\ (-1, \pi - \cos^{-1}(c_{j\nu}^*)) & c_{j\nu}^* < 0. \end{cases} \tag{14}$$

After extracting the angle and sign, we determine if the switching sequence violates dc voltage constraints. For each $j \in \{1, \ldots, r\}$, we sort the elements $(\sigma_{j\nu}, \alpha_{j\nu})$ in increasing order by $\alpha_{j\nu}$ to create a sorted list $(\hat{\sigma}_{j\nu}, \hat{\alpha}_{j\nu})$ with running sum $\hat{\sigma}'_{j\nu} = 0$ and $\hat{\sigma}'_{j\nu} = \sum_{\nu'=1}^{\nu} \hat{\sigma}_{j\nu'}$. The recovered switching sequence may be generated by the multilevel converter if and only if $\|\hat{\sigma}_{j\nu'}\|_\infty \le m_j$ for every $j \in \{1, \ldots, r\}$. We then sum up the switching sequences for each partition into a sequence $\mathcal{T} = (u, \alpha)$ across all partitions.

IV. Numerical Examples

The code is publicly available at the repository https://github.com/jarmill/she_unequal. The SHE solutions were found using Julia, using the libraries `SemialgebraicSets.jl` for symmetry reduction and `HomotopyContinuation.jl` to solve the symmetry-reduced polynomial equations.

A. Three-Cell H-Bridge

The first example involves control of the three-cell converter from Example 2.1 with $E = (2, 2, 3)$.

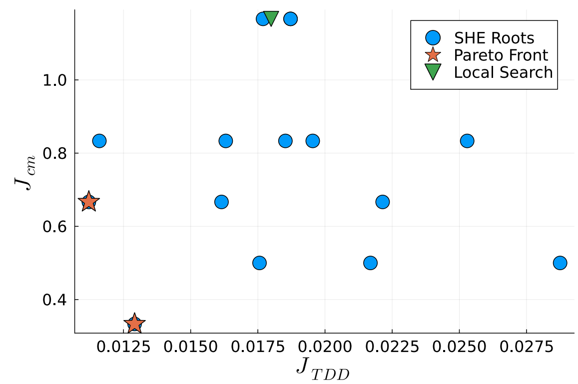

Fig. 3: SHE Pareto front for $E = (2, 2, 3)$, $d = 4$, and $M = 2$

TABLE II: SHE solutions with $E = (2, 2, 3), d = 4, M = 2$

Partition γ	(4, 0)	(3, 1)	(2, 2)	(1, 3)	(0, 4)
# real roots of (12)	6	21	30	21	4
# feasible patterns	0	11	8	6	0
min. J_{TDD}	N/A	1.462%	1.167%	1.313%	N/A
max. J_{TDD}	N/A	3.080%	2.615%	2.976%	N/A
min. J_{cm}	N/A	1/2	2/3	1/2	N/A
max. J_{cm}	N/A	11/6	5/3	3/2	N/A

1) Fixed Amplitude: In a first step, $d = 4$ switching transitions per quarter period are considered, while the amplitude of the desired fundamental voltage component is set to $M = 2$. The harmonics constrained in this SHE problem are $H = (1, 5, 7, 11)$, and the switching partitions are $\gamma \in ((4, 0), (3, 1), (2, 2), (1, 3), (0, 4))$. Solving the elementary-symmetric polynomial SHE system in (12) leads to 82 real solutions across all partitions. Of these real solutions, only 25 lead to feasible pulse patterns. The feasible pulse patterns have a minimum J_{TDD} of 1.167% and a maximum J_{TDD} of 3.080%, in which the differential-mode objective in (6b) is summed up to the maximum harmonic order $\ell = 500$. Table II reports the counts and distortions of recovered pulse patterns at each partition γ. The SHE-feasible pattern that achieves the minimal J_{TDD} of 1.167% was generated by the partition $\gamma = (2, 2)$, is listed in (3), and is visualized in Fig. 2.

Fig. 3 plots the the maximal common-mode voltage (vertical axis) and current TDD (horizontal axis) performance metrics among all the 25 roots in this example (blue circles). The orange stars mark points on the Pareto front between J_{cm} and J_{TDD}; the pattern in (3) is associated to the left-most orange star at $J_{\text{TDD}} = 1.167\%$ and $J_{\text{cm}} = \frac{5}{6}$. A local search among the partitions is also performed, yielding the suboptimal green triangle point with $J_{\text{TDD}} = 1.799\%$ and $J_{\text{cm}} = \frac{7}{6}$. [20].

2) Parameter Sweeps: Subsequently, M is varied from 0.05 to 3.7 in increments of 0.05. Fig. 4 shows the minimum and maximum values of the differential-mode TDD over all feasible patterns for each value of M.

Following, M is fixed to $M = 2$ and the pulse number d is increased from 2 to 7. The number of patterns and TDD values for SHE solutions of this d-sweep are listed in Table III.

3) Impact of DC Source Variations on the Solution Space: To evaluate the robustness and flexibility of the proposed

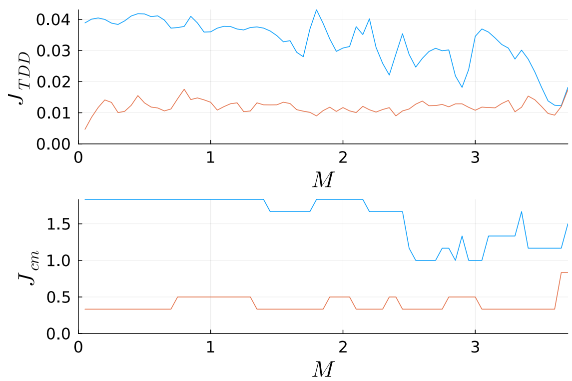

Fig. 4: Minimum and maximum J_{TDD} and J_{cm} vs. M

TABLE III: Patterns and J_{TDD} vs. increasing d

d	# patterns	Min. J_{TDD}	Max. J_{TDD}
2	3	2.496%	6.631%
3	9	1.674%	3.004%
4	25	1.167%	3.078%
5	74	0.999%	2.374%
6	169	0.916%	2.253%
7	369	0.7742%	2.0407%

symmetry-reduced SHE method under a range of operating conditions, the solution space (Pareto fronts) is analyzed across different dc-source asymmetry profiles. For the three-cell CHB converter, the dc voltage vector E is varied to represent different degrees of cell charge imbalance or alternative converter configurations. Specifically, four cases are considered: a slight asymmetry $(1.5, 1.5, 2)$, an equal-source case $(2, 2, 2)$ providing a symmetric baseline with an extended modulation range, the nominal base case $(2, 2, 3)$, and a fully asymmetric case $(1, 2, 3)$.

As the dc levels deviate from the symmetric case, the proposed algebraic framework continues to yield multiple valid switching patterns that satisfy both the fundamental voltage requirement and the targeted harmonic constraints ($H = \{5, 7, 11\}$). However, the distribution of the unconstrained harmonic content changes, giving rise to a distinct Pareto front for each dc-voltage configuration and thereby altering the trade-off between current quality and common-mode voltage stress.

This behavior is visually captured in Fig. 5, which shows the feasible solution space for all four dc profiles at the fixed desired fundamental voltage amplitude $M = 2.0$. The resulting Pareto fronts highlight the trade-off between line current quality, quantified by J_{TDD}, and common-mode voltage, quantified by J_{cm}.

To facilitate a systematic comparison, three representative operating points are selected from the Pareto front of each dc-voltage configuration:

- **Case A (Minimum J_{TDD}):** prioritizes grid code compliance and current quality by selecting the pattern that yields the lowest differential-mode distortion, regardless of the common-mode voltage.
- **Case B (Intermediate Trade-off):** selects a balanced solution near the "knee" of the Pareto front, effectively mitigating the common-mode voltage without incurring a substantial increase the line current distortion.
- **Case C (Minimum J_{cm}):** prioritizes strict mitigation of common-mode voltages to reduce insulation stress and leakage currents, at the expense of a higher distortion in the line current.

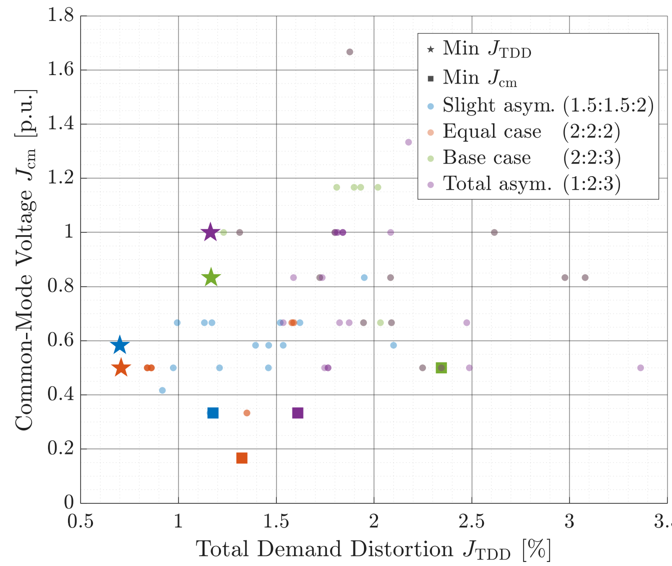

Fig. 5: Pareto fronts of the feasible SHE solution space for $M = 2.0$ for different configurations.. The markers highlight the optimal operating extremes for each evaluated case.

Table IV summarizes the theoretical performance metrics for the considered dc-voltage configurations. An important observation at $M = 2.0$ is the convergence of Case A and Case B across all evaluated configurations. This indicates that, at this operating point, the gradient of the Pareto front is highly non-linear; even a small reduction in common-mode voltage away from the minimum-J_{TDD} solution is accompanied by a comparatively large increase in the current TDD. As a result, the Pareto front provides little separation between the minimum-J_{TDD} point and an intermediate trade-off solution.

Conversely, when the optimization strictly enforces common-mode reduction (Case C), the algorithm successfully identifies alternative algebraic roots that substantially reduce J_{cm}, e.g., from $1.000\,\text{p.u.}$ to $0.333\,\text{p.u.}$ in the fully asymmetric case. This confirms that the multiplicity of SHE solutions can be exploited to shift the operating point according to the desired trade-off between common-mode voltage and current quality.

B. *Five-Cell H-Bridge*

The second example considers the setting in [11] with $E = (1, 0.93, 0.89, 0.84, 0.8)$, $M = 0.8\,\frac{4}{\pi}$, and $d = 5$. This SHE setting gives rise to a total of $\binom{9}{5} = 126$ partitions. The original work in [11] considers only the single partition $\gamma = (1, 1, 1, 1, 1)$, thus restricting each cell to perform one switching transition per quarter period (one switch per cell).

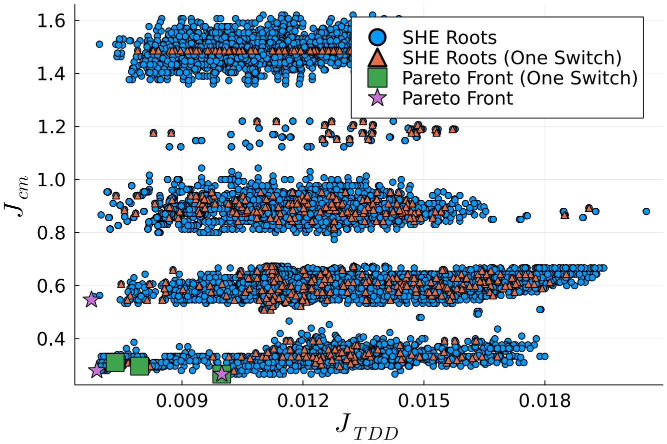

Fig. 6: Pareto front for SHE in a five-cell CHB converter

TABLE IV: Selected SHE performance metrics for $M = 2.0$ across different dc-voltage configurations

E (p.u.)	Case	J_{TDD} (%)	J_{cm} (p.u.)
(1.5, 1.5, 2)	A	0.700	0.583
	B	0.700	0.583
	C	1.177	0.333
(2, 2, 2)	A	0.707	0.500
	B	0.707	0.500
	C	1.324	0.167
(2, 2, 3)	A	1.167	0.833
	B	1.167	0.833
	C	2.344	0.500
(1, 2, 3)	A	1.163	1.000
	B	1.163	1.000
	C	1.610	0.333

We solve the SHE system in (12) across all 126 partitions. There are 7921 SHE patterns across all partitions, of which 592 satisfy the one-switch-per-cell restriction. Fig. 6 shows J_{cm} and J_{TDD} for all SHE roots (blue circles) and for SHE roots corresponding to patterns with one switch per cell (orange triangles). The three green squares indicate the Pareto front under the one-switch-per-cell restriction, whereas the three purple stars indicate the Pareto front across all partitions. In particular, the minimum value of J_{TDD} over all patterns is 0.6754%, whereas imposing the one-switch-per-cell restriction increases the minimum achievable J_{TDD} to 0.7344%.

V. Conclusion

This paper presented a symmetry-reduced method for solving the unequal SHE problem for CHB converters. The method exploits partition-compatible permutation symmetry by grouping switching angles according to identical dc voltage levels and introducing elementary symmetric polynomials within each group. The resulting reduced polynomial systems are solved using homotopy continuation, enabling the computation of all solutions of the unequal SHE equations with improved computational tractability. Numerical results illustrated the set of feasible solutions and the trade-off between common-mode voltage and current TDD through Pareto fronts. Future work will consider experimental validation and further reduction of the computational complexity.

References

[1] J. Song-Manguelle, G. Ekemb, S. Schröder, T. Geyer, J.-M. Nyobe-Yome, and R. Wamkeue, “Analytical expression of pulsating torque harmonics due to PWM drives,” in *Proc. IEEE Energy Convers. Congr. Expo.*, Denver, CO, USA, Sep. 2013, pp. 2813–2820.

[2] IEEE Std 519-2022 (Revision of IEEE Std 519-2014), “IEEE standard for harmonic control in electric power systems,” pp. 1–31, Aug. 2022.

[3] F. Turnbull, “Selected harmonic reduction in static DC—AC inverters,” *IEEE Transactions on Communication and Electronics*, vol. 83, no. 73, pp. 374–378, 1964.

[4] H. S. Patel and R. G. Hoft, “Generalized Techniques of Harmonic Elimination and Voltage Control in Thyristor Inverters: Part I–Harmonic Elimination,” *IEEE Trans. Ind. Appl.*, no. 3, pp. 310–317, 1973.

[5] ——, “Generalized Techniques of Harmonic Elimination and Voltage Control in Thyristor Inverters: Part II — Voltage Control Techniques,” *IEEE Trans. Ind. Appl.*, no. 5, pp. 666–673, 1974.

[6] M. S. Dahidah, G. Konstantinou, and V. G. Agelidis, “A Review of Multilevel Selective Harmonic Elimination PWM: Formulations, Solving Algorithms, Implementation and Applications,” *IEEE Trans. Power Electron.*, vol. 30, no. 8, pp. 4091–4106, 2014.

[7] J. N. Chiasson, L. M. Tolbert, K. J. McKenzie, and Z. Du, “A unified approach to solving the harmonic elimination equations in multilevel converters,” *IEEE Trans. Power Electron.*, vol. 19, no. 2, pp. 478–490, 2004.

[8] C. Wang, Q. Zhang, D. Chen, Z. Li, W. Yu, and K. Yang, “Application of Newton Identities in Solving Selective Harmonic Elimination Problem With Algebraic Algorithms,” *IEEE Journal of Emerging and Selected Topics in Power Electronics*, vol. 10, no. 5, pp. 5870–5881, 2022.

[9] I. G. Macdonald, *Symmetric functions and Hall polynomials*. Oxford university press, 1998.

[10] K. Yang, Q. Zhang, R. Yuan, W. Yu, J. Yuan, and J. Wang, “Selective harmonic elimination with Groebner bases and symmetric polynomials,” *IEEE Trans. Power Electron.*, vol. 31, no. 4, pp. 2742–2752, 2015.

[11] K. Yang, Q. Zhang, J. Zhang, R. Yuan, Q. Guan, W. Yu, and J. Wang, “Unified selective harmonic elimination for multilevel converters,” *IEEE Transactions on Power Electronics*, vol. 32, no. 2, pp. 1579–1590, 2016.

[12] K. Yang, X. Tang, Q. Zhang, and W. Yu, “Unified selective harmonic elimination for fundamental frequency modulated multilevel converter with unequal DC levels,” in *IECON 2016-42nd Annual Conference of the IEEE Industrial Electronics Society*. IEEE, 2016, pp. 3623–3628.

[13] A. J. Sommese, C. W. Wampler *et al.*, *The Numerical solution of systems of polynomials arising in engineering and science*. World Scientific, 2005.

[14] S. Pan, M. Wu, J. Wang, X. Li, Y. W. Li, W. Yu, and K. Yang, “Unified Switching Frequency Minimized Harmonic Mitigation Technique for Asymmetric Cascaded H-Bridge Converters,” *IEEE Journal of Emerging and Selected Topics in Power Electronics*, vol. 12, no. 2, pp. 2006–2016, 2024.

[15] C. Buccella, C. Cecati, and M. G. Cimoroni, “SHE formulation for five level inverters with unequal DC sources,” in *Proc. IEEE Int. Conf. Ind. Technol.* IEEE, 2015, pp. 1167–1172.

[16] G. Schettino, C. Nevoloso, G. Scaglione, R. Miceli, C. Cecati, C. Buccella, and M. Cimoroni, “Novel Selective Harmonic Mitigation Algorithm for Seven-level Three-phase Cascaded H-Bridge Inverters,” in *2024 International Symposium on Power Electronics, Electrical Drives, Automation and Motion (SPEEDAM)*. IEEE, 2024, pp. 889–894.

[17] M. Ahmed, M. Orabi, S. S. Ghoneim, M. M. Al-Harthi, F. A. Salem, B. Alamri, and S. Mekhilef, “General mathematical solution for selective harmonic elimination,” *IEEE J. Emerg. Sel. Top. Power Electron.*, vol. 8, no. 4, pp. 4440–4456, 2019.

[18] B. Wu and M. Narimani, *High-power converters and AC drives*. John Wiley & Sons, 2017.

[19] P. Breiding and S. Timme, “HomotopyContinuation. jl: A package for homotopy continuation in Julia,” in *International Congress on Mathematical Software*. Springer, 2018, pp. 458–465.

[20] M. J. Powell, “A Direct Search Optimization Method That Models the Objective and Constraint Functions by Linear Interpolation,” in *Advances in optimization and numerical analysis*. Springer, 1994, pp. 51–67.